



OPEN ACCESS

EDITED BY

Emmanuel Iheanyichukwu Iwuoha,
University of the Western Cape, South Africa

REVIEWED BY

Abdelghani Benyoucef,
University of Mascara, Algeria
Usisipho Feleni,
University of South Africa, South Africa

*CORRESPONDENCE

Mangaka Matoetoe,
✉ lellangm@gmail.com

RECEIVED 04 March 2024

ACCEPTED 19 August 2024

PUBLISHED 03 October 2024

CITATION

Timakwe S, Ngcobo S, Smith R and Matoetoe M
(2024) Nanoclay composites in
electrochemical sensors.
Front. Sens. 5:1395853.
doi: 10.3389/fsens.2024.1395853

COPYRIGHT

© 2024 Timakwe, Ngcobo, Smith and
Matoetoe. This is an open-access article
distributed under the terms of the [Creative
Commons Attribution License \(CC BY\)](#). The use,
distribution or reproduction in other forums is
permitted, provided the original author(s) and
the copyright owner(s) are credited and that the
original publication in this journal is cited, in
accordance with accepted academic practice.
No use, distribution or reproduction is
permitted which does not comply with these
terms.

Nanoclay composites in electrochemical sensors

Sapokazi Timakwe, Sizwe Ngcobo, Randall Smith and
Mangaka Matoetoe*

Department of Chemistry, Cape Peninsula University of Technology, Cape Town, South Africa

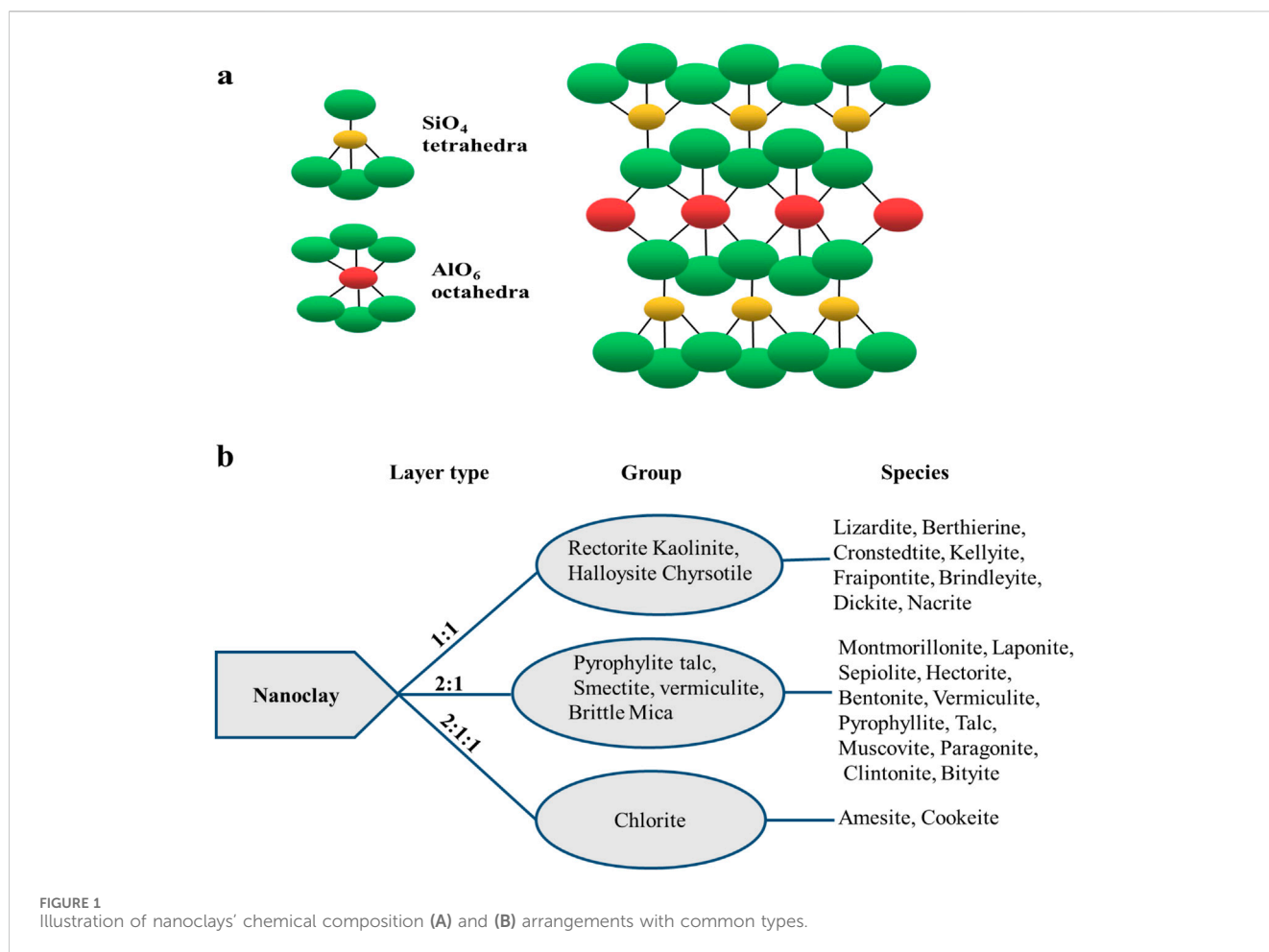
Nanoclays are layered structures in the nanoscale range with widespread application due to their unique properties such as swelling, cation exchange capacity, and ease of functionalisation using metals, metal oxides, and organic compounds such as carbon paste, polymers, and other biomolecules that form nanoclay composites. Nanoclay functionalisation with silver (Ag), zinc oxide (ZnO), and bimetallic silver–gold (Ag–Au) using hydrophilic and hydrophobic clays is here evaluated and discussed. The composites' synthesis and morphological, crystallinity, and electroactive properties in comparison with pure nanoclay are also assessed. The layered structure and crystallinity of all these nanoclay composites were slightly changed. The clumped layered structures on the surface of the nanocomposites had dispersed white spots that indicated possible surface modification. The nano-films of the composites' electroactivity were comparatively high, as seen from the increase in current in the cyclic voltammetry characterisation voltammograms and the differential pulse voltammograms of the pharmaceutical detection. Efavirenz, nevirapine, and zidovudine detection was improved by modification of the nanocomposite with human serum albumin (HSA), as shown by the higher current, thus indicating improved conductivity of the composites compared to the pure nanoclays. Applying HAS-modified nanocomposites in the analysis of efavirenz, nevirapine, and zidovudine on a glassy carbon electrode (GCE) showed good linearity and acceptable detection limits comparable to those of previous studies. Therefore, it has potential for application in pharmaceutical quality control and environmental monitoring.

KEYWORDS

nanoclay, composites, sensors, functionalisation, characterisation

1 Introduction

The applicability of electrochemical sensors is becoming increasingly widespread, driven by improvements in transduction (Chaudhary et al., 2022; Brahimi et al., 2003; Wahyuni et al., 2024). Electrical transduction improvements can be traced back to the inception of nanomaterials and their composites (Maake et al., 2022). The major role of these nanomaterials in electrochemical sensors is in electrode modification. These material-modified electrodes have increased the application of electrochemical sensors as a result of their uniform electrode fabrication procedures, which result in improved response and sensitivity due to their increased surface area, giving them faster kinetics and reproducibility (Bergaya et al., 2013; Mousty, 2004; Huang et al., 2008). Electrochemical sensors are popular due to their versatility, miniaturisation potential, procedural simplicity, fast analysis time, ability to measure complex samples, high sensitivity, and cost-effectiveness (Ghadiri et al., 2015; Okumu et al., 2020; Silwana and Matoetoe, 2022). These advantages have been



augmented by the use of various nanomaterials such as metals, oxides, carbon, polymers, and nanoclays, including their composites. The focus of this study is on nanoclay composites, mainly due to their safety and environmental friendliness (Timakwe et al., 2023; Nisha et al., 2023). Their increasing use is due to their highly specific surface area, poor permeability, swelling ability, chemical and mechanical durability, and high ion sorption/exchange capacity (Timakwe et al., 2023; Savic et al., 2014).

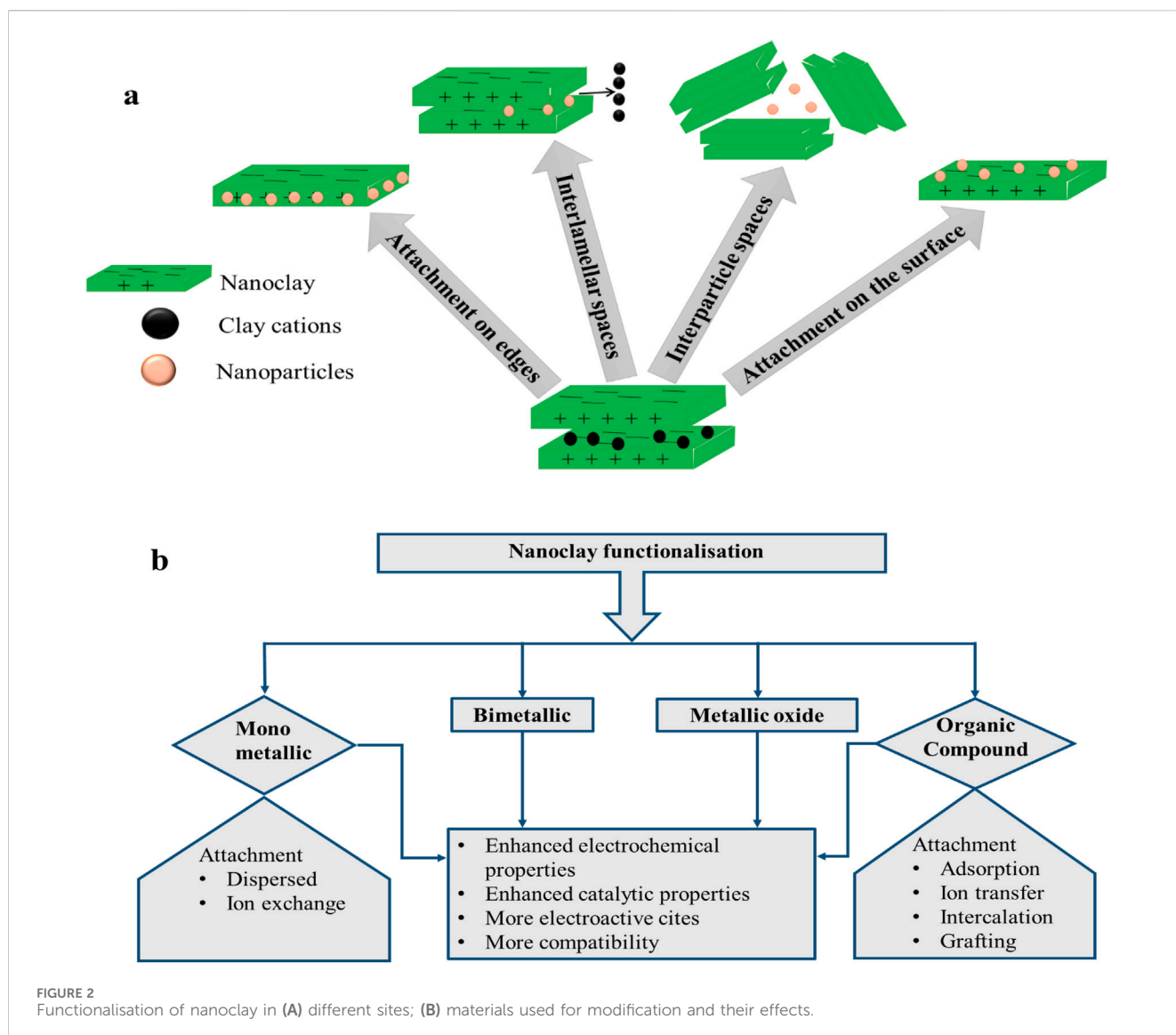
Nanoclays are phyllosilicates made up of SiO₄ tetrahedra polymeric layers joined to (Mg, Fe, and Al) (O, OH)₆ octahedra thin sheets (Figure 1A) (Timakwe et al., 2023; Shetti et al., 2020). A nanoclay sheet's thickness is approximately 1 nm or less, and its size range is 1–100 nm (Guo et al., 2018). The arrangement of the sheets determines the distinguishing aspects of the nanoclays, resulting in approximately 30 different types.

Figure 1B shows the major three octahedral and tetrahedral sheet arrangements: 1:1, 2:1, and 2:1:1. The 1:1 sheet arrangement is one tetrahedral to one octahedral, while 2:1 indicates that each octahedral is bonded to two tetrahedrals. The 2:1:1 is an octahedral sheet bonded to two tetrahedrals and one octahedral (Savic et al., 2014; Majeed et al., 2013; Barton and Karathanasis, 2016).

A variety of nanoclays exist, the commonest of which have a plate-like appearance such as montmorillonite (MMT), while the nanoclay smectite has 10 μm-sized multilayer stacks. The average dimensions of halloysite with aluminosilicate nanotubes are

approximately 15 nm × 1,000 nm (Bergaya et al., 2013). Halloysite nanotubes (HNTs) have an inner and outer diameter smaller than 100 nm and lengths of 0.2–1.5 μm (Garcia-Hernandez et al., 2024). The most popular clay minerals are shown in Figure 1B. Bentonite nanoclays that exist as montmorillonite (MMT) form a large part of the nanoclays studied due to their easily modifiable layered structure, which is held together by weak van der Waals and electrostatic forces (Timakwe et al., 2023; Batista et al., 2019; Zhou et al., 2019). However, the use of nanoclays in electrochemical sensors is hampered by their poor conductivity—hence the dominant use of nanocomposites.

Nanoclay composite formation involves the functionalisation of nanoclay by the incorporation of conductive material/nanoparticles (NPs) to chiefly enhance their conductivity. Some frequently employed materials and attachment modalities for nanoclay functionalisation are represented in Figures 2A, B. Metal or metal oxide can be mechanochemically intercalated into the clay structure (Guo et al., 2018; Song, 2017). There are a number of locations (Figure 2A) on the clay where a species can be adsorbed during the functionalisation of nanoclay, including edge attachment, interlamellar spaces, interparticle spaces, and surface attachment (Timakwe et al., 2023; Shetti et al., 2019a). The method of surface functionalisation preserves the selectivity of the nanoparticles and keeps them from aggregating (Awasthi et al., 2019). Other stable materials that have been incorporated into clay minerals are carbon



nanomaterials, nanocellulose, nanofibers, and silica nanotubes (Cruces et al., 2022). Approximately 90% of the clay's surface comprises the interlayer gap, which allows for the absorption of molecules of water and other substances (Kryuchkova et al., 2021). The interlayer space of montmorillonite clay serves as a support for the binding of transition metal complex catalysts during the creation of materials and biomaterial nanoparticles, as well as an adsorbent for cationic ions (Timakwe et al., 2023).

Functionalising materials can be subdivided into four different categories (Figure 2B). The attributes of these nanocomposites are vital for electrochemical sensors (Fatimah et al., 2022; Pavón et al., 2021; Ngcobo et al., 2022) and are also summarised in Figure 2B. In metal composites, metal nanoparticles are dispersed into the clay structure through an *in situ* dispersion, or ion exchange mechanism, involving metal ions and native cations of the clay mineral (Fatimah et al., 2022).

The cations in clays are readily interchangeable with other cations or molecules due to their exchangeable qualities; hence, they play a part in nanoclay modification (Fatimah et al., 2022).

Smectite (Figure 1B) is the most frequently used group for metal and metal oxide modification, generating efficient composites which enable nanoclay use for oxidation procedures as well as rapid organic reactions (Fatimah et al., 2022; Tan et al., 2023). Moreover, the layered structure, together with the ion exchange process, controls the covalent bonding of the modifier to atoms on the nanoclay sheet (Fatimah et al., 2022). The formation of clay nanocomposites may be achieved by methods including molten state, solution blending, and polymerization; the latter is the most advantageous process due to its ability to create more structural gaps in the particles by widening the spaces between the clay layers, causing the transition of clay mineral from being intercalated to exfoliated (Awasthi et al., 2019).

Various incorporations of metals (Timakwe et al., 2023; Nisha et al., 2023; Awasthi et al., 2019; Pavón et al., 2021; Jlassi et al., 2018), bimetallics (Cruces et al., 2022; Ngcobo et al., 2022), and metal oxides (Fatimah et al., 2022) into nanoclays have resulted in the production of exceptional composite materials of high chemical reactivity, high surface-to-volume ratio, and high electrochemical

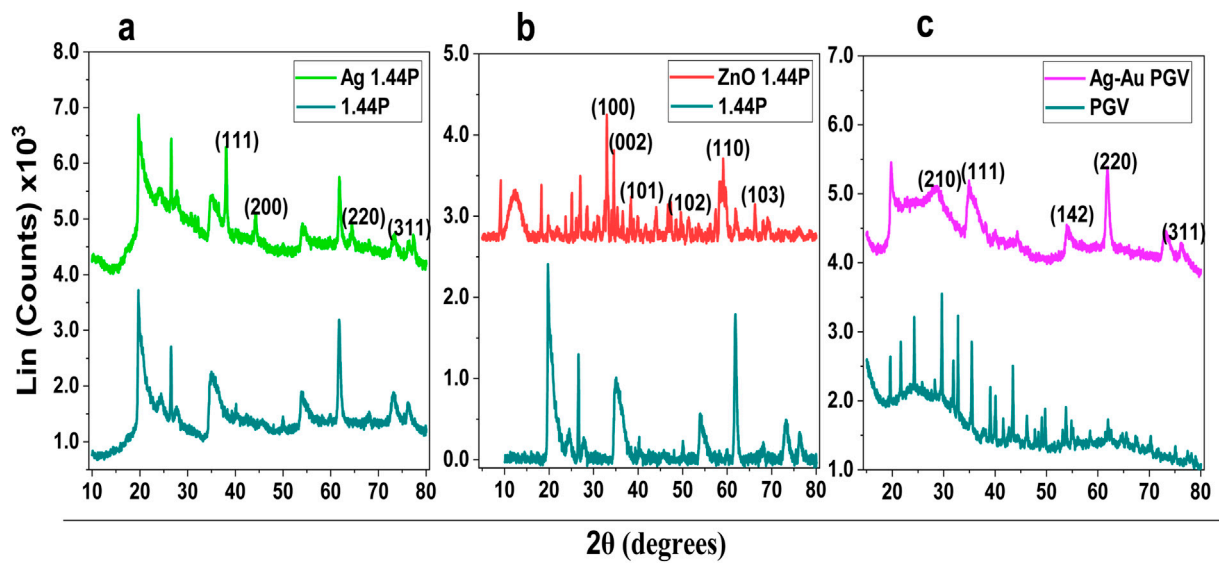


FIGURE 3 XRD of nano clay composites with silver (A), zinc oxide (B), and silver-gold nanoparticles (C).

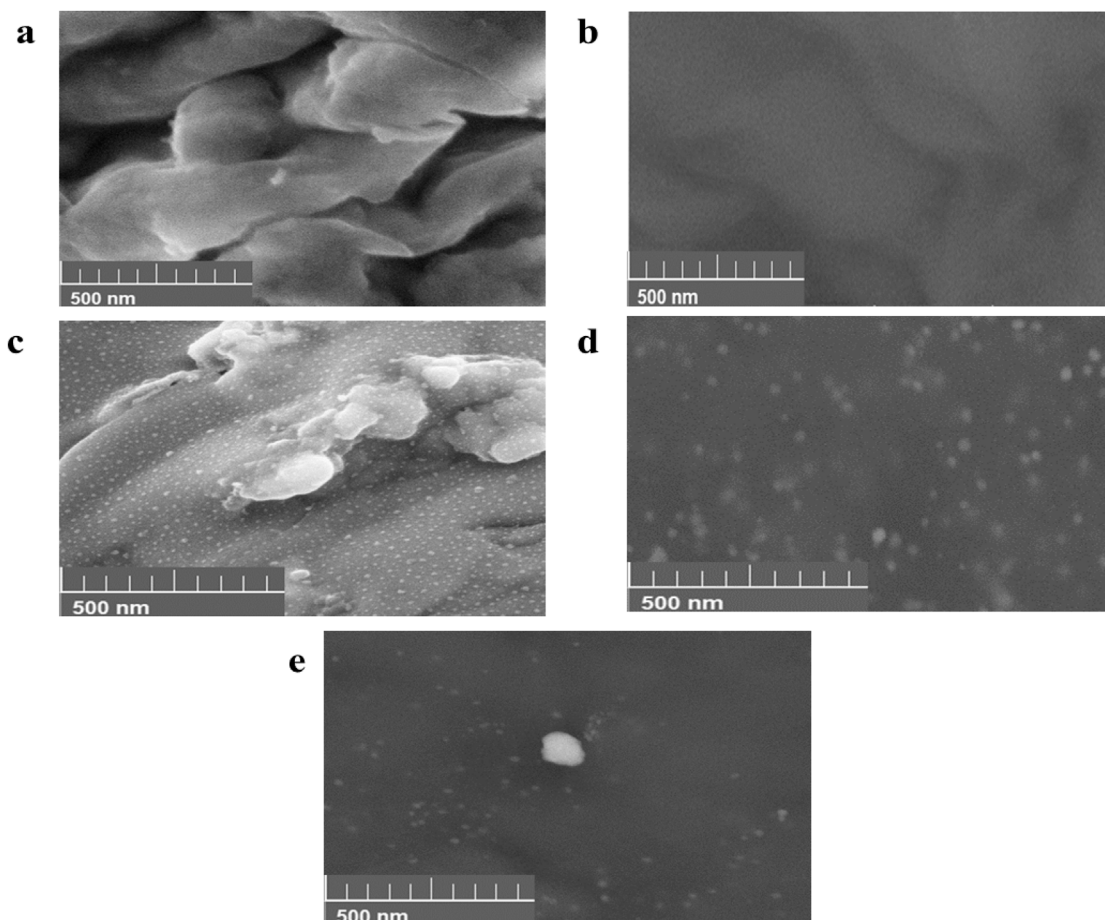


FIGURE 4 Scanning electron micrograph of pure nano clay (A) PGV (B) and 1.44P, and nanocomposites (C) Ag-Au PGV, (D) Ag 1.44P, and (E) ZnO 1.44P.

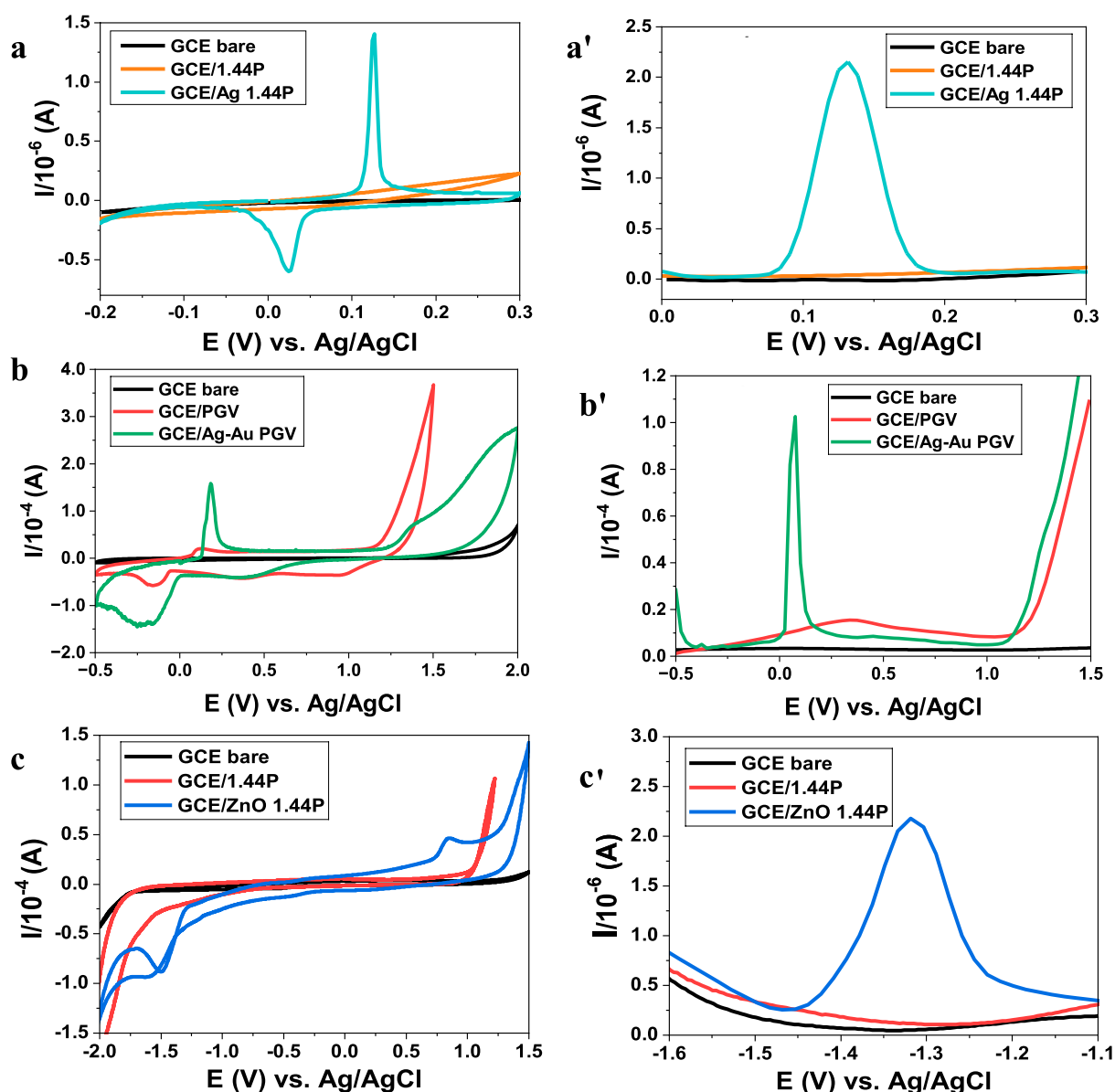


FIGURE 5
 Voltammograms (CV) and (DPV) of nanoclay composites (a,a) Ag/1.44P scan rates 50 mV/s, (b,b), Ag–Au PGV scan rates 30 mV/s, and (c,c) ZnO 1.44P scan rate 30 mV/s in 0.1 M HCl electrolyte.

conductivity, with the ability to chemisorb different types of molecules. In addition, the composites possess improved optical, catalytic, and photocatalytic activities (Timakwe et al., 2023; Sheikh-Mohseni et al., 2020; Wu et al., 2020). These attributes are ideal for environmental and electrochemical sensors (Das et al., 2018). In electrochemical sensors, the incorporation of organic molecules such as methyl viologen (MV), cetyltrimethylammonium (SaCTA), didodecyldimethyl ammonium (SaDDA), and acetylcholinesterase (AChE) (Pavón et al., 2021) into nanoclay promotes the binding of biomolecules. Compatibility and binding improvement on the nanoclay surface can also be achieved by functionalising the composites with compounds such as 3-aminopropyl)triethoxysilane (APTES), glutaraldehyde, and

polyethylene glycol (PEG) (Nisha et al., 2023; Mbokana et al., 2020; Gaharwar et al., 2011), usually resulting in the increased adhesion of cells, spreading, and improved levels of alkaline phosphate (ALP) and mineralised matrix synergy—attributes that are vital in pharmaceutical and bacterial detection.

The use of nanoclay composites in electrochemical sensors is increasing due to their low cost and adaptable matrix, thus offering mechanical and thermal resilience, chemical stability, and ion exchange capabilities which result in better signal transduction (Nisha et al., 2023; Pavón et al., 2021). Due to these distinctive qualities, nanoclays are a desirable material for electrode modification (Vernekar et al., 2020; Killedar et al., 2022; Shetti et al., 2019b). Smectites, which include montmorillonite, laponite,

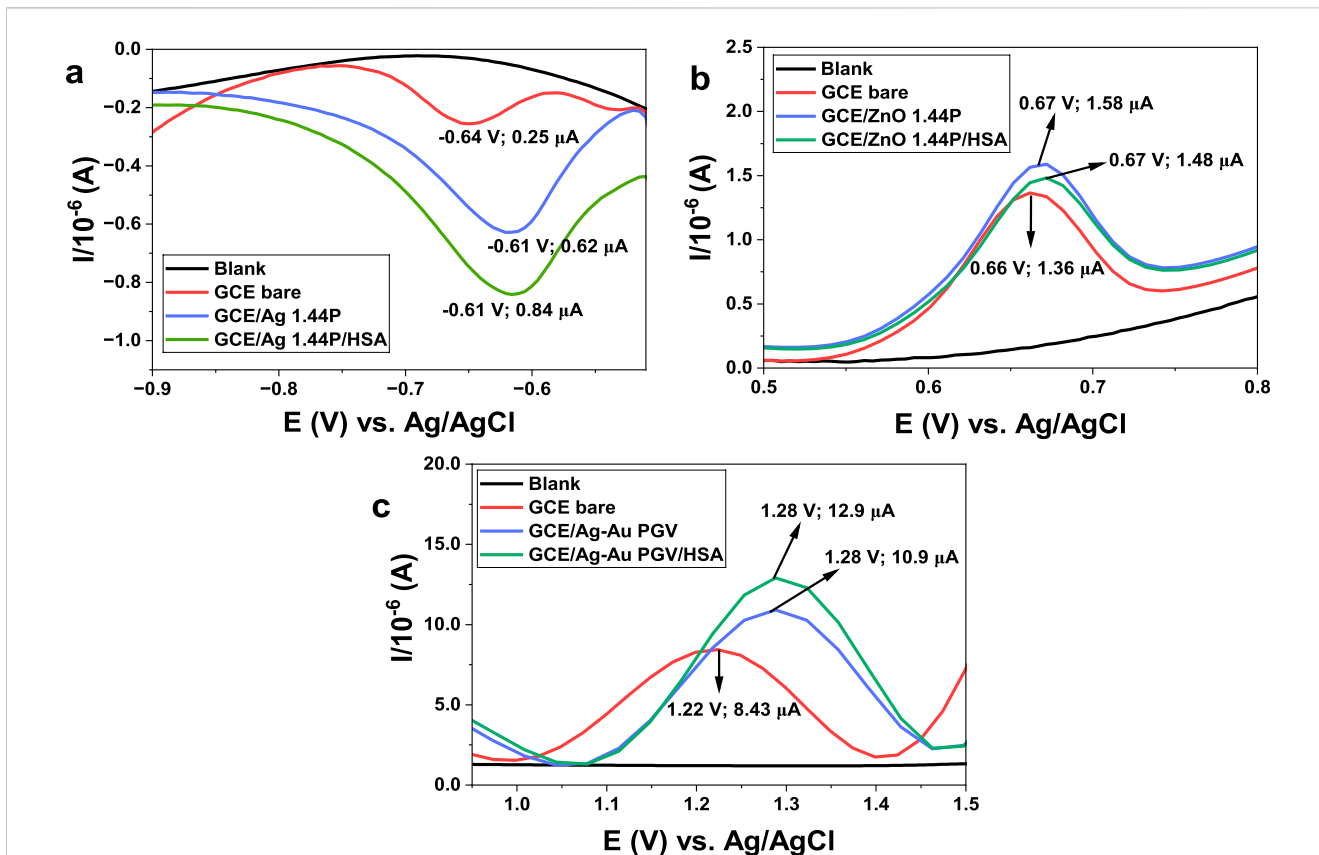
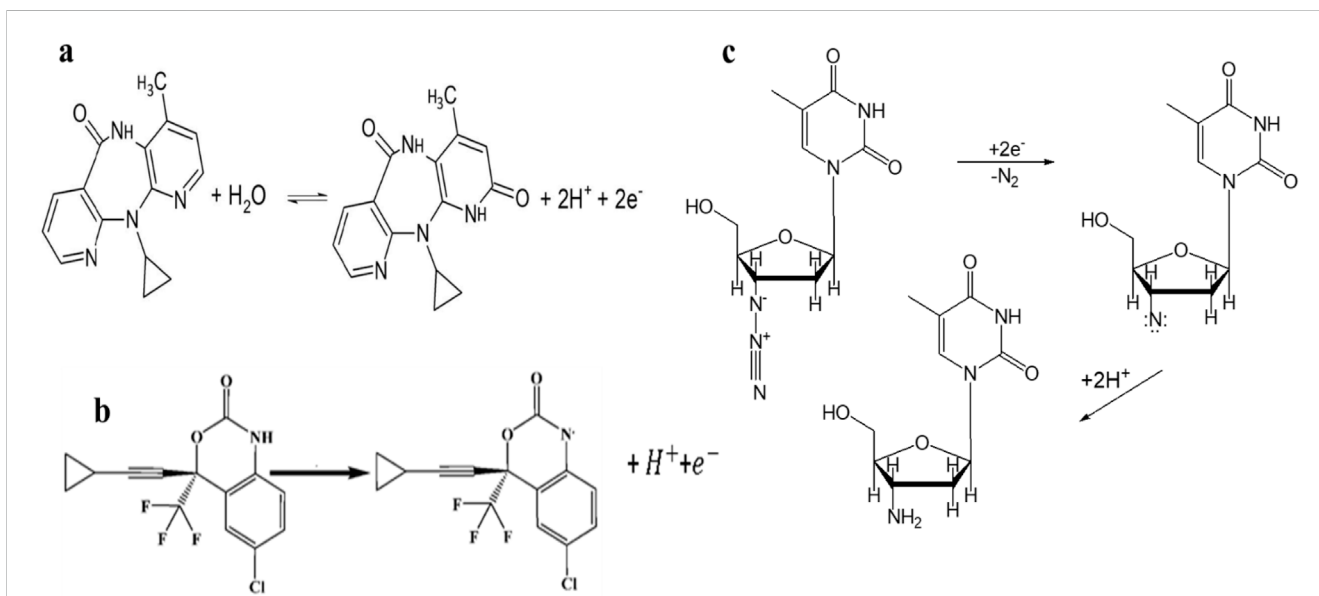


FIGURE 6 Effects of electrode modification with nano clay (1.44P and PGV) and its composites (Ag, ZnO, and Ag–Au) on pharmaceutical detection. (A) DPV of 20.5 μM ZDV using the Ag 1.44P scan rate 50 mV/s. (B) 24.5 μM NVP using ZnO 1.44P, scan rate 30 mV/s. (C) 30.6 μM EFV voltammograms obtained using bimetallic Ag–Au PGV using scan rate 30 mV/s.



MECHANISM 1
Oxidation reaction of NVP (A), EFV (B), and reduction reaction of ZDV (C).

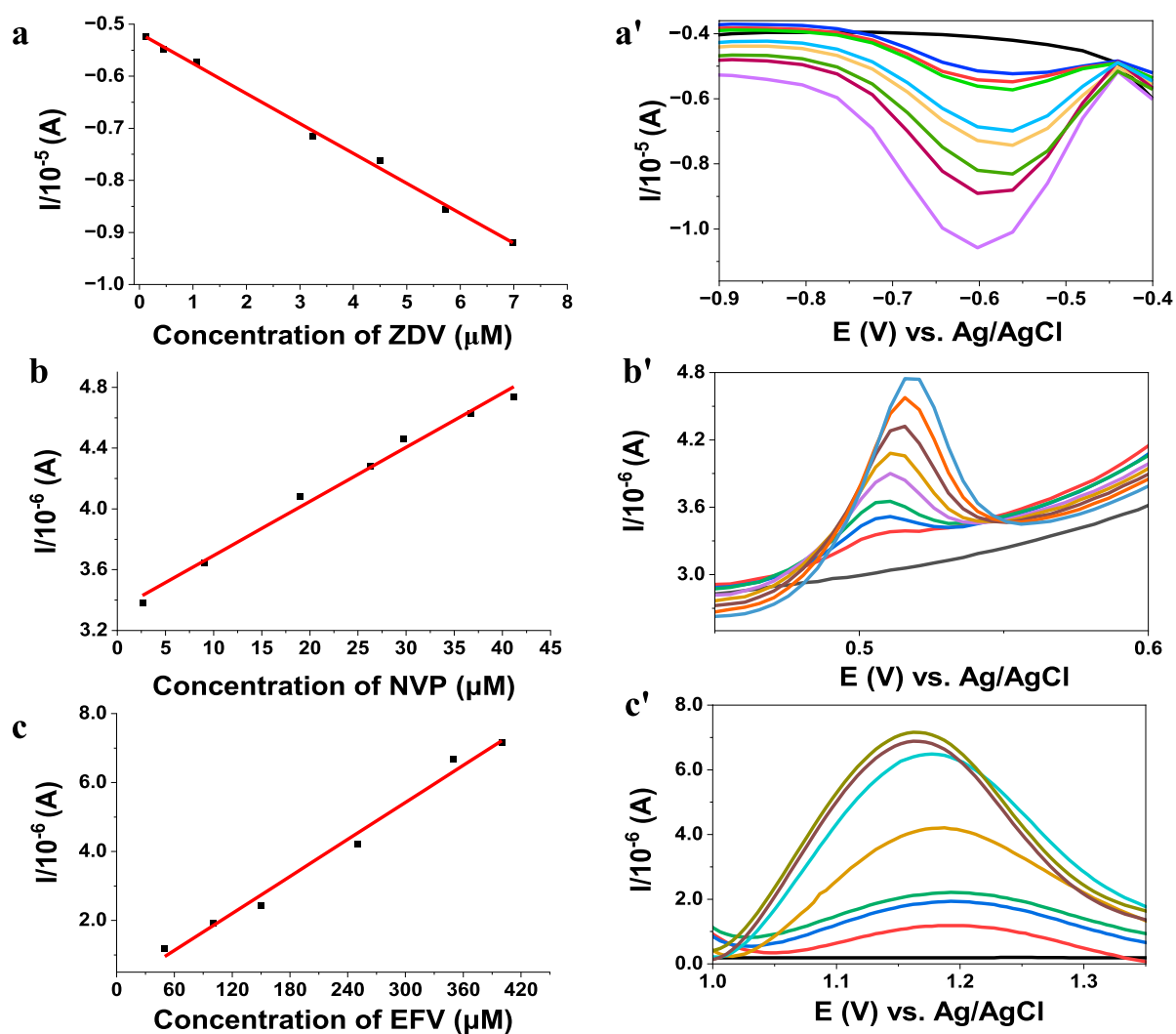


FIGURE 7 Biosensor calibration graph and DPV concentration dependent on voltammograms using phosphate buffer pH 7 (a,a'), Ag 1.44P/HSA detection of zidovudine (scan rate 50 mV) (b,b'), ZnO 1.44P/HSA nevirapine detection and Ag–Au PGV/HSA for the detection of efavirenz (c,c').15 days.

TABLE 1 Comparison of current study with reported studies.

Analyte	Sensor	Clay	Modifier	Technique	Range μM	LOD μM	References
Catechol	PEI/HNT /PEI/Cupc ^{SO₃⁻}	HNT	Cupc ^{SO₃⁻} PEI	CV	10.0–138	0.938	Garcia-Hernandez et al. (2024)
Nimesulide	NC CPE	MMT	CPE	DPV	0.01–0.35	0.001	Shetti et al. (2020)
Cd	Clay/C/AAAPTS	Sepiolite	AAAPTS	ASV	0.02–0.87	0.006	Sheikh Arabi et al. (2019)
Pb	Clay/C/AAAPTS	Sepiolite	AAAPTS	ASV	0.01–0.48	0.005	Sheikh Arabi et al. (2019)
Vanillin	SMM/Au-ZIF-67/CPE	SMM	Au-ZIF-67/CPE	DPV	0.001–1.20	0.003	Dehdashtian et al. (2023)
Mesotrione	Sadda	Smectite	Surfactants	SWV	0.25–2.50	0.260	Wagheu et al. (2013)
Efavirenz	NC/Ag-Au/HSA	Bentonite PGV	Ag-Au-HSA	DPV	1.00–300	0.310	This study
Nevirapine	NC/ZnO/HSA	Bentonite 1.44P	ZnO-HSA	DPV	2.00–38.0	0.390	This study
Zidovudine	NC/Ag/HSA	Bentonite 1.44P	Ag-HSA	DPV	0.12–6.98	0.300	This study

3-[2-(2-aminoethylamino) ethylamino] propyl-trimethoxysilane (AAAPTS); sodium montmorillonite nanoclay (SMM); carbon paste (CPE); carbon (C).

and nontronite, make up the majority of clay minerals used in clay-based sensors and have been used in analytical procedures (Pavón et al., 2021). Nanoclay-based sensors have been utilised for the identification of minute metabolic compounds in bodily fluids at low quantities—primarily glucose, dopamine, and hydrogen peroxide (H_2O_2)—for the early diagnosis of various disorders (Pavón et al., 2021). In an electrochemical sensor, the electroactive surface can be enhanced by the addition of nanoclay, leading to increased responses at the same concentration of the analyte (Nisha et al., 2023). There are reports of the use of electrochemical sensors fabricated with bentonite clay for determining toxic metal ions and pharmaceuticals (Rastogi et al., 2016). Fabrication of an electrochemical sensor made from 2D nanoclay sheets embedding a carbon paste electrode for identifying and quantifying famotidine content in trace levels demonstrated improved stability, repeatability, sensitivity, specificity, and efficiency in biological urine samples (Killedar et al., 2022). Comparative studies on layered and non-layered bentonite nanoclays in sensor fabrication to detect and investigate cetirizine activity using cyclic voltammetry (CV) and differential-pulse voltammetry (DPV) methods showed that layered nanoclay had increased peak currents compared to non-layered nanoclay (Vernekar et al., 2020). Carbon compound nanoclays composed of carbon paste and graphene oxide composites have been utilised in improving the electrocatalytic activity of nimesulide and theophylline, respectively (Shetti et al., 2020). A comparison of the efficiency of several carbon paste nanoclay composite sensors to pure carbon paste in detecting nitrophenol, nifedipine, nimodipine drugs (Reddy and Reddy, 2004), and dinoterb herbicides (Sreedhar et al., 2003) shows a marked improvement in sensitivity. Several pesticides have been analysed using nanoclay composites, such as the use of montmorillonite/carboxy cellulose composites in the analysis of methyl parathion (Pavón et al., 2021). The cation exchange capability of nanoclays makes them useful as host matrices for stabilising various compounds, making it possible to add fluorescent probes, biomolecules functioning as enzymes, or electroactive ions, resulting in composites with excellent qualities for use in sensors (Pavón et al., 2021). Metallic, bimetallic, and metal oxide nanoclays have been extensively used in electrochemical sensors. These qualities can be enhanced by immobilising nanoparticles or biomolecules on the surface region of the sensor, thus aiding in the selective identification of the analyte with increased sensitivity, specificity, accuracy, and catalytic activity (Killedar et al., 2022).

Amine and enzymatic integration into nanoclay composites has been reported to improve selectivity (Pavón et al., 2021; Ghadiri et al., 2014). The electrochemical application of nanoclay composites is here illustrated using the nanoclay composites Ag, Ag–Au, and ZnO. Their structural, morphological, and electrochemical property changes are interrogated in comparison with those of the pure nanoclays using XRD, SEM, CV, and DPV. The composites in combination with human serum albumin (HSA) are used in the pharmaceutical analysis of human immunodeficiency virus (HIV) drugs (efavirenz, nevirapine, and zidovudine). The data obtained compared well with those of other electrochemical sensors of nanoclay composites that have been reported, thus providing a good example of the potential applicability of nanoclay composites in electrochemical sensors.

2 Experimental

2.1 Materials and instruments

The following 99.9% purity materials were purchased from Aldrich: silver nitrate (AgNO_3), trisodium citrate ($\text{Na}_3\text{C}_6\text{H}_5\text{O}_7$), chloroauric hydrate (HAuCl_4), hydrochloric acid (HCl), and the nanoclays monomer nanoclay 1,44P and PGV-bentonite. Others were sourced from Merck, such as zinc nitrate ($\text{Zn}(\text{NO}_3)_2$) (98%) and sodium hydroxide (NaOH) (99%). The HIV drugs (efavirenz, nevirapine, and zidovudine) and human serum albumin (HSA) were also purchased from Sigma Aldrich (US), as well as potassium dihydrogen phosphate (KH_2PO_4) and disodium hydrogen phosphate (Na_2HPO_4). Throughout the studies, solutions were prepared with deionised water purified with a Milli-Q system from Merck.

Spectroscopic characterisation was achieved with x-ray diffraction (XRD) using a Bruker (Germany) AXS D8 Advance diffractometer with Cu–K α radiation over a scanning range 2θ of 10° – 90° at 40 kV and 40 mA. The obtained spectra were compared to the standard JCPDS spectra, and the average crystallite sizes were calculated using the Scherrer equation and presuming the Gaussian profile for the band model Scherrer equation as $D = 0.9\lambda/\beta \cos \theta$, where D is the crystalline size, λ the wavelength of x-ray, β the full width at half maximum of the diffraction peak, and θ is Bragg's angle. The scanning electron microscopy (SEM) images were acquired using a Philips-FEI XL30 ESEM-TMP (Czech Republic). The powdered samples were first affixed onto adhesive tapes supported on metallic disks and then covered with a thin, electric conductive gold film. Images of metals and bentonite nanocomposite were recorded at different magnifications at an operating voltage of 5.0 kV solid form. Approximately 2 mL of the nanoparticles was dropped onto a copper plate. The images were analysed using ImageJ software for size determination.

Electrochemical studies were performed with a typical conventional compartment three-electrode system connected to an Autolab PGSTAT 101 operating in NOVA 2.1 software from Metrohm South Africa. Three electrode cell set-ups consisted of a glassy carbon electrode (GCE), a platinum wire, and an Ag/AgCl electrode. The GCE was polished with 0.05, 0.3, and 1 μm alumina powder to remove any residue deposits on the surface. As part of the daily polishing routine, the GCE was sonicated in water. All measurements were performed after degassing.

2.2 Methods for nanoclay functionalisation/modification

Nanoclay composites of both hydrophobic MMT nanomer nanoclay (1.44P) and hydrophilic MMT nanoclay (PGV) were synthesised using *in situ* chemical reduction of the precursors of silver, zinc oxide, and silver–gold nanoparticles, forming nanoclay composites (Ag 1.44P, ZnO 1.44P, and Ag–Au PGV). The Ag nanoclay composite preparation involved mixing 0.5 g of nanoclay (1.44P) with 1.0 mM silver nitrate solution. The mixture was heated at 240°C to boil with continuous stirring at 265 rpm. After 20 min of stirring, a dropwise addition of 4 mL 0.01 M of trisodium citrate dihydrate in the mixture was made. The mixture was heated for another 15 min and

cooled at room temperature, followed by purification with Milli-Q water through centrifugation. A similar approach was adopted in the preparation of ZnO nanoclay composites, where 0.5 g of the nanoclay (1.44P) was added in 100 mL, 0.2 M solution zinc nitrate in a round-bottomed flask kept at constant heat of 80°C with vigorous stirring. After 15 min of stirring, 10 mL of 1 M NaOH was added dropwise in the mixture that was continuously heated and vigorously stirred. The changes in the reaction were monitored and allowed to proceed for 2 hours. After this period, the mixture was removed from heat and stirred, allowing it to cool to room temperature. The formed product was transferred to amber containers to preserve the quality. The obtained ZnO 1.44P was centrifuged and washed three times with Milli-Q water. The bimetallic Ag–Au nanocomposites were prepared as follows: 1 g of nanoclay (PGV) was dispersed in a 100-mL mixture of 1 mM AgNO₃ and 1 mM HAuCl₄ solutions for 24 h. The Ag–Au PGV-bentonite dispersions were cleaned by centrifugation thrice with pure water and dried at 105°C.

2.3 Electrode modification with nanoclay composites

The GCE was coated at separate times with nanoclay or nanoclay composites (Ag 1.44P, ZnO 1.44P, and Ag–Au PGV). The method that was used to modify the electrode was drop-coating, using approximately 0.5 μL of slurry of the material under study cast on the bare GCE. The modified GCE was left to dry in an open vacuum for 2 h. For the pharmaceutical analysis, the composite nanofilm was modified by drop coating approximately 0.2 μL of 1% HSA, leaving it to stand in the dark for the time dictated by the optimum conditions of the analytes (times ranged from 30 min to 60). The method and electrode modification parameters were optimised for each nanocomposite.

2.3.1 Optimum conditions

Zidovudine: 0.0405 V step potential, 0.075 V modulation amplitude, 0.01 s modulation time, 0.25 s interval time, scan rate 50 mV/s.

Neverapine: scan rates 30 mV/s, 0.035 V step potential, 0.075 modulation amplitude, 0.3 s modulation time, 0.20 s interval time.

Efavirenz: scan rate 30 mV/s, step potential 0.030 mV, modulation amplitude 0.070, and time (modulation 0.25 s, interval 0.20s).

3 Results and discussion

3.1 Nanocomposite characterisation

The XRD spectra of the resulting nanoclay composites (Ag 1.44P; ZnO 1.44P; Ag–Au PGV) are depicted in Figures 4A–C. These spectra consist of characteristic diffraction patterns of the metals which are absent in the spectra of pure nanoclay as well as the additional diffraction patterns that are present in the pure nanoclays. The characteristic diffraction patterns of metals or metal oxides present in the composites were confirmed using the standard JCPDS spectra. The peak intensities were smaller than

those of the pure nanoclay, suggesting larger sizes of the composites. The complex nature of nanoclay (Section 1) complicates their spectra interpretation, especially in the lower 2 θ ranges.

In Figure 3A, the presence of Ag in the nanoclay composites is confirmed by slight crystalline improvement as well as by the presence of Ag theta peaks on the spectra. Similarly, in Figure 3B the presence of Zn from the ZnO shows the characteristic Zn peaks with some crystallinity improvement as the peak width is smaller. However, the bimetallic Au–Ag PGV in Figure 3C, which is a hydrophilic nanoclay, is amorphous compared to the PGV, with a remarkable decrease in peak intensity accompanied by widening peak width. The average crystallite sizes obtained for the composites are Ag 1.44P at 12.42 nm, ZnO 1.44P at 11.45 nm, and Ag–Au PGV at 27.42 nm (Timakwe et al., 2023; Ngcobo et al., 2022).

The SEM images of the two pure nanoclays (PGV and 1.44P) used and the resultant composites (Ag–Au PGV, Ag 1.44P, and ZnO 1.44P) are shown in Figures 4A–E. The pure nanoclay images show smooth surfaces sheets compared to the composites (Figures 4A, B). However, the layers are banded together and appear as lumps, suggesting aggregation. The nanocomposites in Figures 4C–E still show the same morphology as the nanoclay with white evenly dispersed spots on the surface of the lumped sheets. These differences in morphology are more visible for PDV (Figure 4A) and Ag–Au PGV composites (Figure 4C), which are clearer than the hydrophobic nanoclay composites, whose layered structure is obscured by the lumping.

The analysis using ImageJ software showed average sizes of 20.97 nm, 23.45 nm, 9.56 nm, 27.5 nm, and 29.0 nm for PGV, 1.44P, Ag–Au PGV, Ag 1.44P, and ZnO 1.44P, respectively. The histogram distributions not shown indicate the dominance of particles below 10 nm, which might be due to the dominance of the nanoclay. This strongly suggests a surface coating of the nanoclays (Timakwe et al., 2023; Ngcobo et al., 2022).

The voltammetric responses of nanoclay composites (Ag 1.44P, Ag–Au PGV, ZnO 1.44P) and the pure nanoclays are shown in Figures 5A–C. The hydrophobic 1.44P nanoclay (Figures 5A, C) is not electroactive, while the hydrophilic PGV nanoclay is electroactive as it shows an Fe²⁺/Fe³⁺ couple at 0.3 V/0.8 V (Figure 5B). All voltammograms depict distinct electroactivity differences between the nanoclay composites and the pure nanoclays. The nanocomposites' peaks have a higher current compared to the pure nanoclay voltammograms and are thus indicative of increased conductivity. The composites are all electroactive, showing characteristics of the modifying metal/metal oxide. From Figure 5A, Ag 1.44P has an Ag⁺/Ag couple; Figure 5B has four peaks (two anodic and two cathodic) which correspond to Ag⁺/Ag and Au³⁺/Au couples. There is a slight shift of the peak potentials of these couples and a higher Ag⁺/Ag couple current. These observations are similar to those of reported Ag–Au NP bimetallic studies (Ngcobo et al., 2022; Rastogi et al., 2016). The ZnO 1.44P composites in Figure 5C show the reduction of ZnO at approximately 1.27 V followed by the oxidation of the Zn²⁺ around –1.5 V. Similar behaviour for the ZnO NPs was reported by Smith et al. (2023). This current conductivity improvement may be due to improved dispersion and intercalation as seen in the SEM images. The increase in the electrochemical response of the composites is a crucial characteristic favoured in the development of sensors for various applications (Timakwe et al., 2023).

3.2 Nanocomposites' electrochemical sensors and biosensors

3.2.1 Confirmation of analyte interaction with nanoclay composites

The detection of the analytes zidovudine, nevirapine, and efavirenz on the nano-surface of human serum albumin (HSA) on modified and non-modified nanoclay composites was interrogated using DPV (Figures 6A–C). The signal responses of these three pharmaceuticals increased in the current, accompanied by a positive potential shift, compared to the bare electrode response in Figures 6A–C. The voltammograms obtained using the HAS-modified and -unmodified nanocomposites had the same potentials. However, HAS-modified nanoclay composites resulted in higher currents (Figures 6A–C). They also resulted in higher analyte responses produced in the presence of HAS, thus indicating improved conductivity, catalytic, or amplification functions of the composite nanofilms. There is also a possibility of increased analytic sites on the composites. The HAS higher currents can also be a result of improved compatibility. HAS-modified nanocomposites were more reproducible than the nonmodified nanocomposites. The ZnO 1.44P (Figure 6B) composites show the slight changes in peak current with the addition of HAS compared to other nanoclay composites. These might be attributed to the inactivity of oxides.

HAS-modified nanofilms are also more stable than the chemical nanofilms and were hence adopted for the sensors. Possible redox reactions taking place on the surface of the electrodes are summarised in Mechanism 1. Two reactions (NVP and ZDV) involve two electron transfers, while the reaction of efavirenz involves one electron transfer. Nevirapine and efavirenz undergo oxidation while zidovudine undergoes reduction.

3.2.2 Analysis of efavirenz, nevirapine, and zidovudine

HAS-modified nanoclay composites were chosen as examples to show the pharmaceutical application of nanoclay composites. The optimal conditions for each nanocomposite electrode modification and analyte detection were obtained and used to ascertain the analytical parameters of each analyte. The HAS-modified Ag 1.44P, ZnO 1.44P, and Ag–Au PGV calibrations and different concentration voltammograms for the detection and quantification of ZDV, NVP, and EFV are shown in Figure 7.

There, the analysis is displayed in a linear graph, with r^2 of 97–99 from efavirenz to zidovudine with a <2% error for all of them. The validity of these methods was assessed using recovery studies in aqueous and biological media (diluted urine) which all ranged from 95% to 102% for all three different dilutions. The detection limits obtained were 0.310 μM , 0.390 μM , and 0.300 μM for efavirenz, nevirapine, and zidovudine, respectively. Under optimum conditions, the selectivity, reproducibility, and electrode stability of the studies were evaluated and found to be acceptable. However, interference results obtained with an electrode fabricated 10 days prior show a marked interference in the presence of other HIV drugs studied. The content of the analyte of interest is significantly increased (>10% increase), while the studied supplements did not present any observable interferences (changes <5%) when present in large amounts.

These HIV drugs are the cause of some of the new reported environmental problems as a result of their common use, hence their recent detection in surface water bodies (Kairigo et al., 2020; Ndube et al., 2018). Therefore, HIV monitoring techniques are vital in environmental control and production quality control, thus ensuring quality products.

The measurements were performed after oxygen removal; the calibration graphs obtained for these studies are shown in Figure 7. The analytical parameters of these biosensors were compared with the literature (Table 1).

Although the biosensors reported here have more unfavourable analytical parameters than other reported work on similar analytes, sensors and biosensors remain the favoured analytical techniques due to the minimum sample preparation required. Recently, Pavón et al. (2021) reviewed the recent trends in nanoclay composites in sensors, highlighting the effects of the combination of nanotechnology and widespread use of nanoclay-modified electrodes in electrochemical sensors for detecting pesticides, glucose, hydrogen peroxide, organic acids, proteins, and bacteria. This indicates how nanoclay composites have become a key factor in sensor development and their potential in creating a possible emerging technology for the detection of bioanalyses, with both environmental and biomedical application.

These materials responded well in the analysis of commercial pills/capsules. However, these data need validation since these samples contain chemicals which were not part of the interference studies. Their application in wastewater samples will also be assessed after potential interference in such samples are tested. These samples contain chemicals such as binders, starch, other pharmaceuticals like antibiotics, and pesticides. There is hence a need to assess the interference of these chemicals prior to analysis. The other important issue in real sample analysis is the preservation of the samples.

4 Conclusion

All the nanoclay composites studied show improved catalytic activity, thermal stability, and conductivity. The morphological and crystallinity changes of the composites may have an effect in the improved electroactivity, which may have affected the roughness of the modified electrode as well as improved the electron transfer rates. The surface area enhancements may also have resulted in increased active sites. Extensive use of the nanoclay composites is explained by the observed structure, morphology, and electroactivity of the nanoclay composites. Therefore, the data confirm the potential of nanoclay usage in electrochemical sensors and explain the observed changes as due to changes in the morphology and adaptation of the modifying metals/metal oxides as their electroactive properties are maintained in the composite. The composites have acceptable low detection limits, and hence have potential application in HIV pharmaceutical analysis. The hydrophobic modifiers were more stable than the hydrophilic modifiers.

Data availability statement

The raw data supporting the conclusions of this article will be made available by the authors, without undue reservation.

Author contributions

ST: formal analysis, investigation, and writing—original draft. SN: data curation, formal analysis, investigation, and writing—original draft. RS: data curation, formal analysis, investigation, and writing—original draft. MM: conceptualization, funding acquisition, supervision, and writing—review and editing.

Funding

The authors declare that no financial support was received for the research, authorship, and/or publication of this article.

Acknowledgments

The authors acknowledge the National Research Foundation (NRF) (Grant no. 116237) of South Africa and Cape Peninsula University of Technology for their financial support; iThemba labs and University of Cape Town respectively for access to XRD and

References

- Awasthi, A., Jadhao, P., and Kumari, K. (2019). Clay nano-adsorbent: structures, applications and mechanism for water treatment. *SN Appl. Sci.* 1, 1076. doi:10.1007/s42452-019-0858-9
- Barton, C. D., and Karathanasis, A. D. (2016). "Clay minerals," in *Encycl. Soil sci.* (Guelph, Canada: Taylor and Francis), 27.
- Batista, F. A., Nascimento, S. Q., Sousa, A. B., Júnior, E. F. R., de Almeida Pereira, P. I., Fontenele, V. M., et al. (2019). Synthesis, characterization and electrochemical properties of composites synthesized from silver-tannic acid hybrid nanoparticles and different clays. *Appl. Clay Sci.* 181, 105219. doi:10.1016/j.clay.2019.105219
- Bergaya, F., and Lagaly, G. (2013). "General introduction: clays, clay minerals, and clay science," in *Handb. Clay sci.* Editors F. Bergaya and G. Lagaly (Amsterdam: Elsevier), 1–19.
- Brahim, S., Wilson, A. M., Narinesingh, D., Iwuoha, E., and Guiseppi-Elie, A. (2003). Chemical and biological sensors based on electrochemical detection using conducting electroactive polymers. *Microchim. Acta* 143, 123–137. doi:10.1007/s00604-003-0065-6
- Chaudhary, V., Kaushik, A., Furukawa, H., and Khosla, A. (2022). Review—towards 5th generation AI and IoT driven sustainable intelligent sensors based on 2D MXenes and borophene. *ECS Sensors Plus* 1, 013601. doi:10.1149/2754-2726/ac5ac6
- Cruces, E., Arancibia-Miranda, N., Manquian-Cerda, K., Perreault, F., Bolan, N., Azócar, M. I., et al. (2022). Copper/silver bimetallic nanoparticles supported on aluminosilicate geomaterials as antibacterial agents. *ACS Appl. Nano Mater.* 5, 1472–1483. doi:10.1021/acsnm.1c04031
- Das, T. K., Ganguly, S., Bhawal, P., Remanan, S., Mondal, S., and Das, N. C. (2018). Mussel inspired green synthesis of silver nanoparticles-decorated halloysite nanotube using dopamine: characterization and evaluation of its catalytic activity. *Appl. Nanosci.* 8, 173–186. doi:10.1007/s13204-018-0658-3
- Dehdashtian, S., Wang, S., Murray, T. A., Chegeni, M., Rostamnia, S., and Fattahi, N. (2023). Determination of vanillin in different food samples by using SMM/Au@ZIF-67 electrochemical sensor. *Sci. Rep.* 13, 17907–17911. doi:10.1038/s41598-023-45342-6
- Fatimah, I., Fadillah, G., Yanti, I., and Doong, R. A. (2022). Clay-supported metal oxide nanoparticles in catalytic advanced oxidation processes: a review. *Nanomaterials* 12, 825. doi:10.3390/nano12050825
- Gaharwar, A. K., Schexnailder, P. J., Kline, B. P., and Schmidt, G. (2011). Assessment of using Laponite® cross-linked poly(ethylene oxide) for controlled cell adhesion and mineralization. *Acta Biomater.* 7, 568–577. doi:10.1016/j.actbio.2010.09.015
- Garcia-Hernandez, C., Garcia-Cabezon, C., Rodriguez-Mendez, M. L., and Martin-Pedrosa, F. (2024). Effect of nanoclays on the electrochemical performance of LbL catechol sensors. *Electrochim. Acta* 476, 143717. doi:10.1016/j.electacta.2023.143717
- Ghadiri, M., Chrzanowski, W., Lee, W. H., and Rohanizadeh, R. (2014). Layered silicate clay functionalized with amino acids: wound healing application. *RSC Adv.* 4, 35332–35343. doi:10.1039/c4ra05216a
- Ghadiri, M., Chrzanowski, W., and Rohanizadeh, R. (2015). Biomedical applications of cationic clay minerals. *RSC Adv.* 5, 29467–29481. doi:10.1039/c4ra16945j
- SEM equipment; And the L'Oréal-UNESCO For Women in Science South African National Program together with the Council for Scientific and Industrial Research (CSIR) for student support.
- Guo, F., Aryana, S., Han, Y., and Jiao, Y. (2018). A review of the synthesis and applications of polymer-nanoclay composites. *Appl. Sci.* 8, 1696–1729. doi:10.3390/app8091696
- Huang, J., Liu, Y., Hou, H., and You, T. (2008). Simultaneous electrochemical determination of dopamine, uric acid and ascorbic acid using palladium nanoparticle-loaded carbon nanofibers modified electrode. *Biosens. Bioelectron.* 24, 632–637. doi:10.1016/j.bios.2008.06.011
- Jlassi, K., Zavahir, S., Kasak, P., Krupa, I., Mohamed, A. A., and Chehimi, M. M. (2018). Emerging clay-aryl-gold nanohybrids for efficient electrocatalytic proton reduction. *Energy Convers. Manag.* 168, 170–177. doi:10.1016/j.enconman.2018.04.109
- Kairigo, P., Ngumba, E., Sundberg, L.-R., Gachanja, A., and Tuhkanen, T. (2020). Contamination of surface water and river sediments by antibiotic and antiretroviral drug cocktails in low and middle-income countries: occurrence, risk and mitigation strategies. *Water* 12, 1376. doi:10.3390/w12051376
- Killedar, L. S., Vernekar, P. R., Shanbhag, M. M., Shetti, N. P., Malladi, R. S., Veerapur, R. S., et al. (2022). Fabrication of nanoclay-modified electrodes and their use as an effective electrochemical sensor for biomedical applications. *J. Mol. Liq.* 351, 118583. doi:10.1016/j.molliq.2022.118583
- Kryuchkova, M., Batasheva, S., Akhatova, F., Babaev, V., Buzyurova, D., Vikulina, A., et al. (2021). Pharmaceuticals removal by adsorption with montmorillonite nanoclay. *Int. J. Mol. Sci.* 22, 9670. doi:10.3390/ijms22189670
- Maake, P. J., Mokoena, T. P., Bolokang, A. S., Hintsho-Mbita, N., Tshilongo, J., Cummings, F. R., et al. (2022). Fabrication of AgCu/TiO₂ nanoparticle-based sensors for selective detection of xylene vapor. *Mater. Adv.* 3, 7302–7318. doi:10.1039/d2ma00587e
- Majeed, K., Jawaid, M., Hassan, A., Abu Bakar, A., Abdul Khalil, H. P. S., Salema, A. A., et al. (2013). Potential materials for food packaging from nanoclay/natural fibres filled hybrid composites. *Mater. Des.* 46, 391–410. doi:10.1016/j.matdes.2012.10.044
- Mbokana, J. G. Y., Dedzo, G. K., and Ngameni, E. (2020). Grafting of organophilic silane in the interlayer space of acid-treated smectite: application to the direct electrochemical detection of glyphosate. *Appl. Clay Sci.* 188, 105513. doi:10.1016/j.clay.2020.105513
- Mousty, C. (2004). Sensors and biosensors based on clay-modified electrodes - new trends. *Appl. Clay Sci.* 27, 159–177. doi:10.1016/j.clay.2004.06.005
- Ndube, S., Madikizela, L. M., Chimuka, L., and Nindi, M. M. (2018). Environmental fate and ecotoxicological effects of antiretrovirals: a current global status and future perspectives. *Water Res.* 145, 231–247. doi:10.1016/j.watres.2018.08.017
- Ngcobo, S., Silwana, B., Maqhashu, K., and Matoetoe, M. C. (2022). Bentonite nanoclay optoelectrochemical property improvement through bimetallic silver and gold nanoparticles. *J. Nanotechnol.* 2022, 1–9. doi:10.1155/2022/3693938
- Nisha, A., Bhardwaj, R., Verma, M., and Acharya, A. (2023). "Functionalized nanoclays in bioactive materials," in *Compos. Interfaces*, 1–25. doi:10.1080/09276440.2023.2291591

- Okumu, F. O., Silwana, B., and Matoetoe, M. C. (2020). Application of MWCNT/Ag-Pt nanocomposite modified GCE for the detection of nevirapine in pharmaceutical formulation and biological samples. *Electroanalysis* 32, 3000–3008. doi:10.1002/elan.202060374
- Pavón, E., Martín-Rodríguez, R., Perdigón, A. C., and Alba, M. D. (2021). New trends in nanoclay-modified sensors. *Inorganics* 9, 43. doi:10.3390/inorganics9060043
- Rastogi, P. K., Yadav, D. K., Pandey, S., Ganesan, V., Sonkar, P. K., and Gupta, R. (2016). Synthesis and characterization of gold nanoparticles incorporated bentonite clay for electrocatalytic sensing of arsenic(III). *J. Chem. Sci.* 128, 349–356. doi:10.1007/s12039-016-1039-7
- Reddy, T. M., and Reddy, S. J. (2004). Differential pulse adsorptive stripping voltammetric determination of nifedipine and nimodipine in pharmaceutical formulations, urine, and serum samples by using a clay-modified carbon-paste electrode. *Anal. Lett.* 37, 2079–2098. doi:10.1081/al-200026681
- Savic, I. M., Stojiljkovic, S., Savic, I., and Gajic, D. (2014). “Industrial application of clays and clay minerals,” in *Clays clay miner. Geol. Orig. Mech. Prop. Ind. Appl.*, 379–402.
- Sheikh Arabi, M., Karami, C., and Ghanei-Motlagh, M. (2019). Fabrication of a novel electrochemical sensor for simultaneous determination of toxic lead and cadmium ions. *Ann. Mil. Heal. Sci. Res.* 17. doi:10.5812/amh.99082
- Sheikh-Mohseni, M. H., Sedaghat, S., Derakhshi, P., and Safekordi, A. (2020). Green bio-synthesis of Ni/montmorillonite nanocomposite using extract of *Allium jesdianum* as the nano-catalyst for electrocatalytic oxidation of methanol. *Chin. J. Chem. Eng.* 28, 2555–2565. doi:10.1016/j.cjche.2020.04.017
- Shetti, N. P., Malode, S. J., Bukkitgar, S. D., Bagihalli, G. B., Kulkarni, R. M., Pujari, S. B., et al. (2019a). Electro-oxidation and determination of nimesulide at nanosilica modified sensor. *Mater. Sci. Energy Technol.* 2, 396–400. doi:10.1016/j.mset.2019.03.005
- Shetti, N. P., Malode, S. J., Nayak, D. S., Bagihalli, G. B., Reddy, K. R., Ravindranadh, K., et al. (2019b). A novel biosensor based on graphene oxide-nanoclay hybrid electrode for the detection of Theophylline for healthcare applications. *Microchem. J.* 149, 103985. doi:10.1016/j.microc.2019.103985
- Shetti, N. P., Malode, S. J., Nayak, D. S., Bukkitgar, S. D., Bagihalli, G. B., Kulkarni, R. M., et al. (2020). Novel nanoclay-based electrochemical sensor for highly efficient electrochemical sensing nimesulide. *J. Phys. Chem. Solids* 137, 109210. doi:10.1016/j.jpccs.2019.109210
- Silwana, B., and Matoetoe, M. C. (2022). Review—nanostructured electrochemical sensors for determination of the first generation of the NNRTIs for HIV-1. *ECS Adv.* 1, 046502. doi:10.1149/2754-2734/ac9323
- Smith, R., Silwana, B., and Matoetoe, M. C. (2023). Electrochemical properties modulation of Zinc oxide nanoparticles. *J. Indian Chem. Soc.* 100, 101054. doi:10.1016/j.jics.2023.101054
- Song, K. (2017). Micro- and nano-fillers used in the rubber industry. *Prog. Rubber Nanocomposites*, 41–80. doi:10.1016/B978-0-08-100409-8.00002-4
- Sreedhar, M., Reddy, T. M., Sirisha, R. K., and Reddy, S. R. J. (2003). Differential pulse adsorptive stripping voltammetric determination of dinoseb and dinoterb at a modified electrode. *Anal. Sci.* 19, 511–516. doi:10.2116/analsci.19.511
- Tan, Y., Yang, Q., Zheng, M., Sarwar, M. T., and Yang, H. (2023). Multifunctional nanoclay-based hemostatic materials for wound healing: a review. *Adv. Healthc. Mater.* 13, 2302700. doi:10.1002/adhm.202302700
- Timakwe, S., Silwana, B., and Matoetoe, M. C. (2023). The impact of silver nanoclay functionalisation on optical and electrochemical properties. *RSC Adv.* 13, 2123–2130. doi:10.1039/d2ra06549e
- Vernekar, P. R., Shetti, N. P., Shanbhag, M. M., Malode, S. J., Malladi, R. S., and Reddy, K. R. (2020). Novel layered structured bentonite clay-based electrodes for electrochemical sensor applications. *Microchem. J.* 159, 105441. doi:10.1016/j.microc.2020.105441
- Wagheu, J. K., Forano, C., Besse-Hoggan, P., Tonle, I. K., Ngameni, E., and Mousty, C. (2013). Electrochemical determination of mesotrione at organoclay modified glassy carbon electrodes. *Talanta* 103, 337–343. doi:10.1016/j.talanta.2012.10.068
- Wahyuni, W. T., Putra, B. R., Rahman, H. A., Ivandini, T. A., Irkham, N., Khalil, M., et al. (2024). Effect of aspect ratio of a gold-nanorod-modified screen-printed carbon electrode for carbaryl detection in three different samples of vegetables. *ACS Omega* 9, 1497–1515. doi:10.1021/acsomega.3c07831
- Wu, K., Li, W., Zhao, S., Chen, W., Zhu, X., Cui, G., et al. (2020). Cobalt tuned copper sulfide on montmorillonite: peroxidase-like activity, catalytic mechanism and colorimetric sensing of hydrogen peroxide. *Colloids Surfaces A Physicochem. Eng. Asp.* 602, 125063. doi:10.1016/j.colsurfa.2020.125063
- Zhou, C., Tong, D., and Yu, W. (2019). “Smectite nanomaterials: preparation, properties, and functional applications,” in *Nanomater. From clay miner. A new approach to green funct. Mater.*, 335–364. doi:10.1016/B978-0-12-814533-3.00007-7